

A finite volume framework for flow in karstified porous media

Fabricio S. Sousa¹, Uebert G. Moreira¹, Franciane F. Rocha²

¹*Institute of Mathematical and Computer Sciences, University of São Paulo
Av. Trabalhador São-carlense, 400, 13566-590, São Carlos, SP, Brazil
fsimeoni@icmc.usp.br, uebert.moreira@usp.br*

²*WIKKI Brasil Consultoria em Engenharia LTDA
Rua Aloísio Teixeira, 278, Prédio 3 - sala 301, Ilha da Cidade Universitária, Rio de Janeiro, 21941-850, RJ, Brazil
fr:franciane@alumni.usp.br*

Abstract. Karst conduit systems exhibit complex geometries, where networks of channels, cavities, or vugs coexist within a porous matrix. Accurately simulating fluid flow in such heterogeneous environments remains a challenge that often limits the reliability of predictions. This study presents a conservative finite volume framework that ensures mass conservation while coupling the karst conduit and porous matrix domains to simulate coupled 1D/3D flows in carbonate rocks. The method is designed to handle intricate networks of karst conduits, including cases in which individual branches have distinct properties - particularly differing permeabilities and size ratios. The karst subdomain is embedded within the matrix grid to ensure geometric consistency and alignment, while mass exchange between the two domains is governed by a transmissibility factor. Numerical experiments include a sensitivity analysis of key parameters, such as permeability contrast and branch ratio, to examine their effects on pressure and velocity fields and to assess the model's ability to capture these variations.

Keywords: Finite volume method, Heterogeneous porous media, Karst conduits, Fluid flow simulations.

1 Introduction

Modeling fluid flow in karstified porous media poses significant challenges due to the intrinsic multiscale heterogeneity and geometric complexity of these systems. Particularly, karst reservoirs are characterized by highly permeable conduit networks - comprising channels, cavities, and vugs - embedded within a less permeable porous rock matrix. This dual-structure configuration results in strongly coupled flow dynamics and sharp contrasts in hydraulic properties, as investigated by Ferraz et al. [1] and Landim et al. [2]. Consequently, accurately representing conduit-matrix interactions is crucial for predictive modeling in applications such as contaminant transport and hydrocarbon recovery.

Several modeling strategies have been proposed to address this complexity. Classical modeling strategies, including equivalent porous media approximations and dual-porosity or dual-permeability models, simplify the geometric and hydraulic diversity observed in real karst systems. However, this can often struggle to capture the explicit geometric and hydraulic variability of conduit networks. These limitations are particularly pronounced in cases involving spatially variable geometries and highly contrasting conduction properties across the domains. To address this, hybrid-dimensional approaches have emerged, wherein the conduits are represented as one-dimensional (1D) entities embedded within a three-dimensional (3D) matrix domain (Murad et al. [3], Correia et al. [4]). These methods seek a balance between geometric fidelity and computational efficiency, simulating the dominant physical processes while managing model complexity. Despite recent advances, ensuring local mass conservation and accurately modeling the interface between domains with strongly contrasting properties remains a key challenge, particularly when the conduit network exhibits significant spatial variability in geometry and permeability.

In this study, we consider a conservative finite volume framework for simulating coupled 1D/3D flow in karstified carbonate formations. To apply the method, our approach embeds the conduit network within the matrix grid, ensuring geometric alignment and local mass conservation. Fluid exchange between the 1D and 3D domains is governed by a transmissibility analytical formulation originally introduced by Cordazzo et al. [5] and further applied in Correia et al. [6] and Correia et al. [4]. The governing system is derived from Darcy's law, assuming single-phase, incompressible flow in both matrix and conduit domains. The discretization is carried out using

the finite volume scheme presented in Moreira et al. [7], that guarantees local mass conservation for karst-matrix coupling. As a reference solution, we employ the FEniCSx platform, an open source computing environment to solve partial differential equations using finite element and finite volume methods (Langtangen and Logg [8]). The choice of FEniCSx is motivated not only by its flexibility and high-performance capabilities but also by its increasing adoption in recent literature addressing flow in fractured and karstified media (e.g., Dudun and Feng [9]).

A sensitivity analysis is conducted to investigate the influence of key physical parameters on the coupled flow behavior. Specifically, we examine the effects of varying the conduit radius and the permeability contrast between the karst conduits and the surrounding matrix. Two simplified geometrical configurations are considered: a horizontal channel and an inclined conduit intersecting the domain at an oblique angle. These configurations, inspired by the study in Zhang et al. [10], allow for a controlled assessment of the model’s capacity to capture essential flow features under varying geometrical and physical conditions. The numerical experiments yield insights into the resulting pressure fields and velocity distributions, contributing to the understanding of hybrid-dimensional flow behavior in heterogeneous karst environments, offering a foundation for future studies in more complex karst structures.

The next section details the mathematical model for coupled karst-matrix flow. Section 3 is dedicated to numerical simulations and their analysis. Lastly, Section 4 provides conclusions.

2 Mathematical model for coupled karst-matrix flow

The conduit is embedded within a structured 3D matrix mesh, and its representation is reduced to a 1D entity aligned with its centerline, as shown in Figure 1. This dimensional reduction significantly lowers computational costs while preserving the ability to capture key flow features. Finite volume cells are constructed to maintain geometric and topological consistency across the coupled domains, ensuring accurate interface representation and mass transfer modeling.

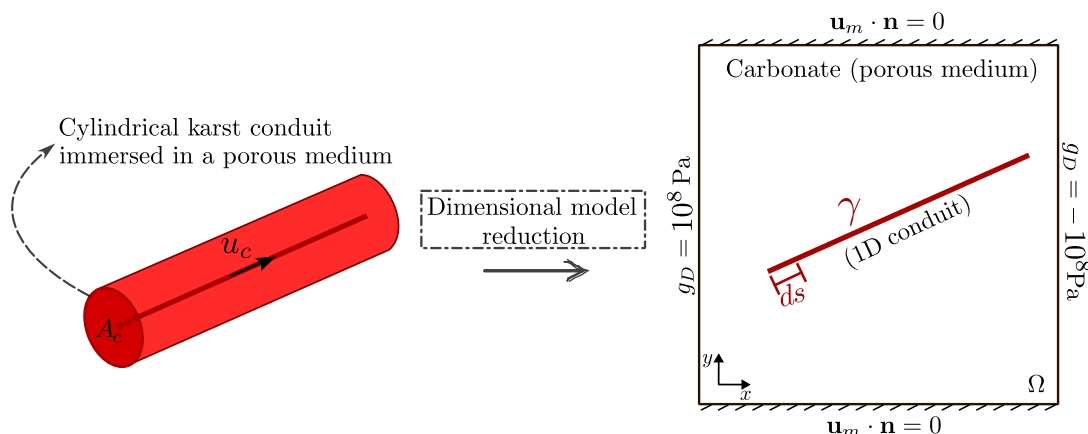


Figure 1. Illustration of the lower dimensional model reduction of the karst conduit.

The mathematical formulation adopted in this work follows a hybrid-dimensional modeling approach for incompressible single-phase flow in karstified carbonate formations. The computational domain $\Omega \subset \mathbb{R}^3$, consists of a porous matrix intersected by a one-dimensional conduit $\gamma \subset \Omega$, which represent the reduced geometry of the karst network. In this setting, flow within both the matrix and the conduits is governed by Darcy’s law, with coupling conditions defined along their intersection.

The model assumes steady-state conditions and neglects gravitational and inertial effects. The porous matrix is described by an elliptic system for the pressure $p_m(\mathbf{x})$ and Darcy velocity $\mathbf{u}_m(\mathbf{x})$, while the flow in the conduit is governed by the pressure $p_c(s)$ and the average axial flux $u_c(s)$, with \mathbf{x} denoting the spatial matrix position and s denoting the coordinate along the conduit centerline. Fluid exchange between the two domains is modeled by an interface term proportional to the pressure difference $(p_c - p_m)$, scaled by the Karst Index (K_I) in the concept presented in Murad et al. [3]. This index generalizes the concept of the classical Well Index (Wolfsteiner et al. [11]), but is computed locally at matrix-conduit intersections, allowing for spatial variation in interface conditions, acting as a parameter similar to transmissibility. We have adopted the transmissibility between the karst conduit element - with side wall area available for mass exchange A_L and length L_c - and the surrounding matrix volume

of edge length L_m , calculated using a two-point flux approximation (TPFA) scheme. This approach is consistent with the formulation presented by Cordazzo et al. [5] and is analytically described as follows:

$$K_I = \frac{2A_L}{(L_m/K_m) + (L_c/K_c)}, \quad (1)$$

where K_m e K_c are the intrinsic permeabilities of the matrix and the conduit, respectively. Although this formulation is based on harmonic means which are consistent with linear flow assumptions, no analytical expression for the Karst Index under fully radial flow conditions is currently available. Given the very small radius of the conduit with homogenized flow effects, TPFA-based transmissibility can be considered as an approximation. Such strategy was employed by Correia et al. [4], who approximated the geometry of the conduit as prismatic to apply the relation (1) in a karst flow context. Despite its linearized nature, eq. (1) provides a practical way to represent matrix-conduit exchange in simulations involving domains with different dimensions. Future works include investigating the calculation of transmissibility terms, taking into account the flow behavior with radially increasing flow area and nonlinear variation of pressure, and studies to obtain estimates based on empirical approaches.

The governing system reads:

$$\begin{aligned} \nabla \cdot \mathbf{u}_m &= \frac{K_I}{\mu} (p_c - p_m) \delta_{cm} + q \delta_m, & \text{in } \Omega, \\ \mathbf{u}_m &= -\frac{K_m}{\mu} \nabla p_m, & \text{in } \Omega, \\ \frac{du_c}{ds} &= -\frac{1}{A_c} \frac{K_I}{\mu} (p_c - p_m), & \text{in } \gamma, \\ u_c &= -\frac{K_c}{\mu} \frac{dp_c}{ds}, & \text{in } \gamma. \end{aligned} \quad (2)$$

In this system, μ denotes the fluid viscosity; q is a source term; A_c is the conduit cross-sectional area illustrated in Figure 1; and δ_{cm} e δ_m are Dirac measures representing mass exchange and external sources. The boundary conditions consist of prescribed pressures ($p_m = g_D$) on the left and right faces of Ω , and homogeneous Neumann conditions on the remaining boundaries ($\mathbf{u}_m \cdot \mathbf{n} = 0$, where \mathbf{n} denotes the unity normal vector pointing outwards to Ω).

To approximate this coupled 3D/1D system, we adopt a finite volume discretization on a structured Cartesian mesh, where each control volume in the matrix and each segment of the conduit are treated independently (Moreira et al. [7]). The interaction between the 3D matrix and the 1D conduit is handled through dedicated coupling terms at the interface locations. In particular, fluxes are computed using harmonic averaging across cell interfaces, and the matrix-conduit exchange is modeled via a transmissibility factor encoded in the Karst Index, allowing spatially varying flow exchange proportional to the pressure difference. A schematic representation of this discretization strategy is provided in Figure 2 (left) to show how the mesh settings are.

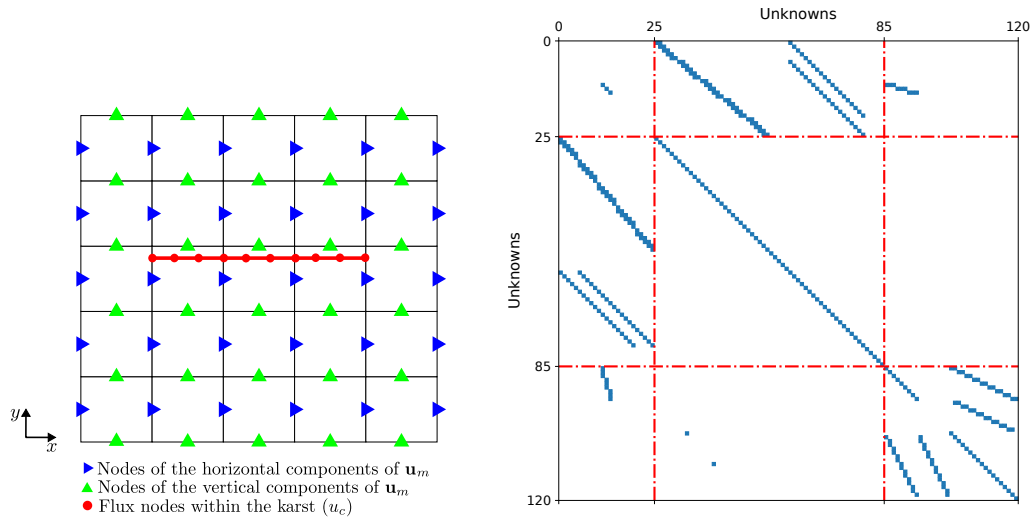


Figure 2. Example of a discretized domain with $5 \times 5 \times 1$ matrix cells and 9 conduit cells (left); the matrix system configuration (right).

The algebraic system resulting from this discretization exhibits a block structure that reflects the separation between the different groups of unknowns. Figure 2 (right) illustrates the nonzero structure of the global system matrix assembled for the horizontal conduit configuration in the sense of the discretization presented in Figure 2 (left). Each block corresponds to interactions among distinct sets of variables in sequence (left to right, top to bottom): pressure unknowns, Darcy velocities in the matrix (horizontal and vertical components) and unknowns associated to conduit fluxes. The red dashed lines indicate the partitioning of the global system, highlighting the sparsity and locality of couplings introduced by the discretization strategy. The off-diagonal extremal blocks represent the matrix-conduit interaction.

This discretization approach retains the conservative nature of the governing equations and is well-suited for structured grids and hybrid-dimensional settings. It also enables straightforward incorporation of geometrical variability, such as changes in conduit radius and orientation, which are essential to the sensitivity analysis conducted in this study.

An important contribution of this work lies in the geometric treatment of the conduit–matrix interface. Rather than homogenizing over coarse domains or adopting a global Karst Index derived from separate experiments, as in our previous work (Moreira et al. [12]), the proposed approach enables localized control of exchange dynamics and improved alignment with realistic geological structures.

3 Results and discussion

We consider a box domain $\Omega = [0, 1] \times [0, 1] \times [0, 0.1] \text{ m}^3$, representing a porous medium intersected by a karst conduit. The fluid is assumed incompressible, and the flow regime is governed by Darcy’s law throughout the entire domain. A high-permeability cylindrical region models the conduit, embedded within a low-permeability matrix. The permeability inside the conduit is fixed at $K_c = 10^{-7}$, while the surrounding matrix permeability K_m and the conduit radius r_c are varied across different simulations to assess the sensitivity of the solution to these parameters. The dynamic viscosity is taken as $\mu = 10^{-3} \text{ Pa}\cdot\text{s}$. Pressure boundary conditions are imposed as $g_D = 10^8 \text{ Pa}$ on the left boundary and $g_D = -10^8 \text{ Pa}$ on the right boundary, while no-flow conditions are enforced on the remaining faces.

The results of this study are compared with numerical solutions obtained using the FEniCSx open-source framework, widely recognized for its robustness in simulating mixed-dimensional flow problems (Langtangen and Logg [8]). In this work, FEniCSx serves as a high-fidelity reference to assess the accuracy of the finite volume approach. This code resolves the entire domain $\Omega_T = \Omega \cup \gamma$, with the conduit explicitly represented as a refined cylinder. In the mixed finite element formulation, the velocity field is discretized using first-order Raviart–Thomas (RT1) elements, which guarantee the continuity of the normal flux across inter-element boundaries. The pressure field is approximated using a discontinuous Galerkin space of zero order (DG0), providing a piecewise constant representation.

The simulations focus on two simplified configurations for the conduit: a horizontal segment aligned with the x -axis and an inclined one forming an oblique trajectory in the x - y plane. The conduit is positioned at the geometric center of the domain with respect to the z -axis. Figure 3 illustrates the computational mesh adopted when $r_c = 10^{-3}$. Although the mesh is adapted when the conduit radius changes, its overall structure and refinement strategy remain consistent with the configuration shown in this figure. The computational meshes used for generating solutions are: the meshes employed for the FEniCSx solution in Figure 3(a), and the simplified Cartesian meshes in Figure 3(b). In both instances, the conduit is highlighted within the meshes to illustrate its representation. In the reduced-dimensional model, where the conduit is represented as a one-dimensional entity, a single cell is used along the z -direction.

For the horizontal configuration, the high-permeability conduit is positioned within the porous matrix along the x -axis, with endpoints at $(0.25, 0.55, 0.05)$ and $(0.75, 0.55, 0.05)$. Simulated pressure and velocity fields computed using both FEniCSx and the finite volume scheme are shown in Figure 4 considering parameters $r_c = 10^{-3}$ and $K_m = 10^{-5}$: Figure 4(a) presents the pressure field for FEniCSx (left) and the finite volume method (right); Figure 4(b) shows the corresponding velocity fields. The finite element meshes consists of 133,817 unstructured tetrahedral elements, while the finite volume formulation employs a structured Cartesian grid of $90 \times 90 \times 1$ cells for the matrix and 138 elements for the conduit. These visualizations provide qualitative results that support the assessment of the finite volume method’s accuracy against a well-established numerical solution, corroborating its good representation when capturing the effects generated by the presence of the high permeability channel. In agreement with Rocha et al. [13], permeability contrasts of this magnitude, especially in binary fields, tend to exert a dominant influence on the flow when compared to cases involving more gradual transitions, reinforcing the expectation that the finite volume framework will work reliably under highly heterogeneous conditions.

For the sensitivity analysis, we investigate the influence of two key parameters: the permeability contrast between the conduit and the surrounding matrix, and the conduit radius. The permeability contrast was varied

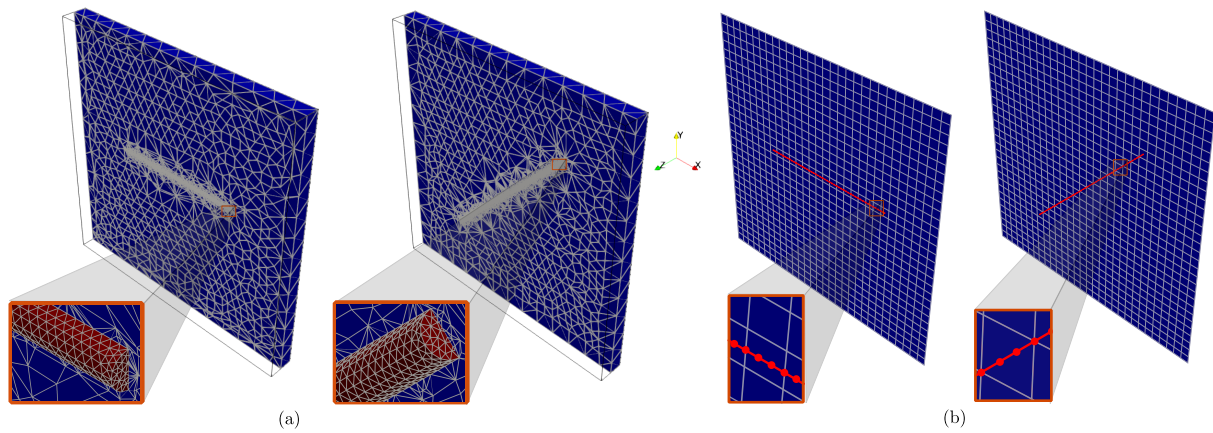


Figure 3. Computational meshes for generating solutions: (a) for the FEniCSx solution and (b) for the simplified formulation.

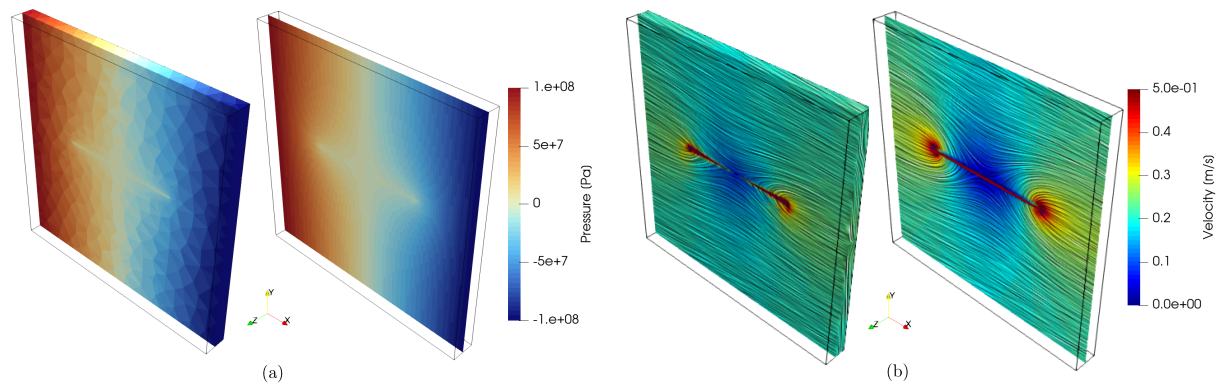


Figure 4. Pressure (a) and velocity (b) fields for a horizontal conduit: obtained by FEniCSx (left) and by the finite volume framework (right).

across six orders of magnitude by adjusting the matrix permeability, while the conduit radius was modified to be commensurate with the dimensions of a Cartesian grid computational cell. Specifically, we considered $K_m \in \{10^{-8}, 10^{-9}, 10^{-10}, 10^{-11}, 10^{-12}, 10^{-13}\}$ and $r_c \in \{5 \times 10^{-4}, 1 \times 10^{-3}, 2 \times 10^{-3}, 3 \times 10^{-3}, 4 \times 10^{-3}, 5 \times 10^{-3}\}$. To isolate the effect of each parameter, two sets of simulations were performed: in one, $K_m = 10^{-12}$ was fixed while r_c varied; in the other, $r_c = 10^{-3}$ was fixed while K_m varied.

Results for the horizontal conduit are summarized in Figure 5 where continuous lines correspond to FEniCSx solutions and dashed lines to those from the finite volume formulation. Both approaches capture a consistent pressure drop near the conduit ends. The finite volume solution exhibits slightly smoother pressure decay for some cases whereas the FEniCSx solution presents sharper variations. The effects of the conduit radius become more significant as its value approaches the grid cell size, consistent with the increased numerical difficulty in representing multi-scale features. In cases with high permeability contrast, the pressure drop becomes more pronounced across both methods, suggesting that the simulations are more sensitive to changes in permeability contrast than to variations in conduit radius. Nevertheless, further cases are required to generalize this observation. Overall, the model reliably reproduces flow behavior associated with permeability contrasts up to 10^6 .

In the oblique configuration, the conduit extends diagonally in the x - y plane, with endpoints at $(0.25, 0.25, 0.05)$ and $(0.75, 0.75, 0.05)$, allowing an assessment of the method's capability to handle non-aligned geometries while maintaining a single computational layer in the z -direction. Figure 6 shows the pressure and velocity fields for this case, using the same parameters as before ($r_c = 10^{-3}$ and $K_m = 10^{-5}$). The FEniCSx mesh includes 131,497 unstructured elements, whereas the finite volume discretization consists of a structured $90 \times 90 \times 1$ grid and 138 conduit elements. Qualitative agreement between both methods remains satisfactory, with key flow features, such as the pressure and velocity field along the conduit, well reproduced. Pressure profiles in Figure 7 show that both

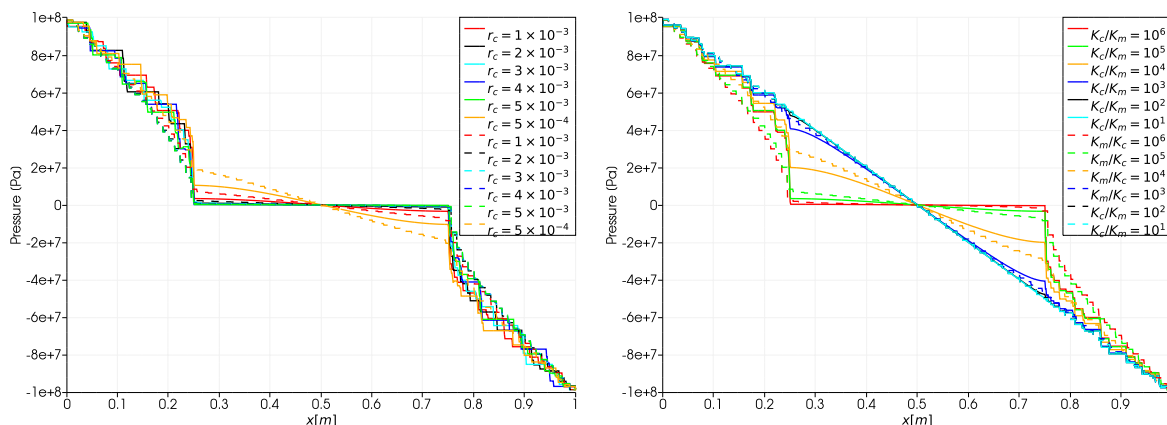


Figure 5. Pressure curves in a horizontal direction for the horizontal conduit. Pressure distribution is shown for varying conduit radius (left) and permeability contrast (right). Continuous lines indicate the FEniCSx solutions, and dashed lines represent the finite volume formulation solutions.

methods capture the overall pressure decay. The differences are more noticeable for small r_c , where sharper drops are observed in the FEniCSx solution. For variations in permeability contrast, successfully captures the dominant flow behavior up to contrast of order 10^6 , reinforcing its applicability high-contrast flow scenarios, even in non-aligned conduit geometries.

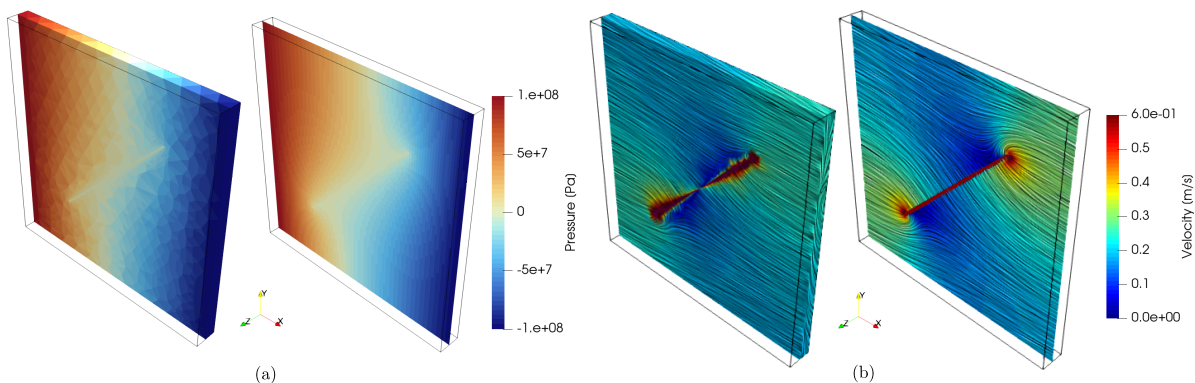


Figure 6. Pressure (a) and velocity (b) fields for an oblique conduit: obtained by FEniCSx (left) and by the finite volume framework (right).

4 Conclusions

The results obtained for both horizontal and oblique conduit configurations confirm that the finite volume approach can reliably reproduce the dominant flow patterns associated with high-permeability channels embedded in a porous matrix. Although minor discrepancies arise when compared to the FEniCSx reference, particularly for small conduit radii or near the conduit-matrix interface, both methods yield qualitatively consistent pressure and velocity fields. The similarity of outcomes across geometrically distinct scenarios suggests that the finite volume formulation remains robust even under non-axis-aligned configurations. These findings support the use of simplified, lower-dimensional representations of conduits in structured meshes for modeling flow in karstified systems, while also highlighting the need for further refinement in capturing localized interfacial dynamics.

Acknowledgements. We acknowledge the financial support from CAPES (Code 001). FSS acknowledges the financial support of FAPESP (grant 2013/07375-0) and CNPq (grant 312372/2023-0).

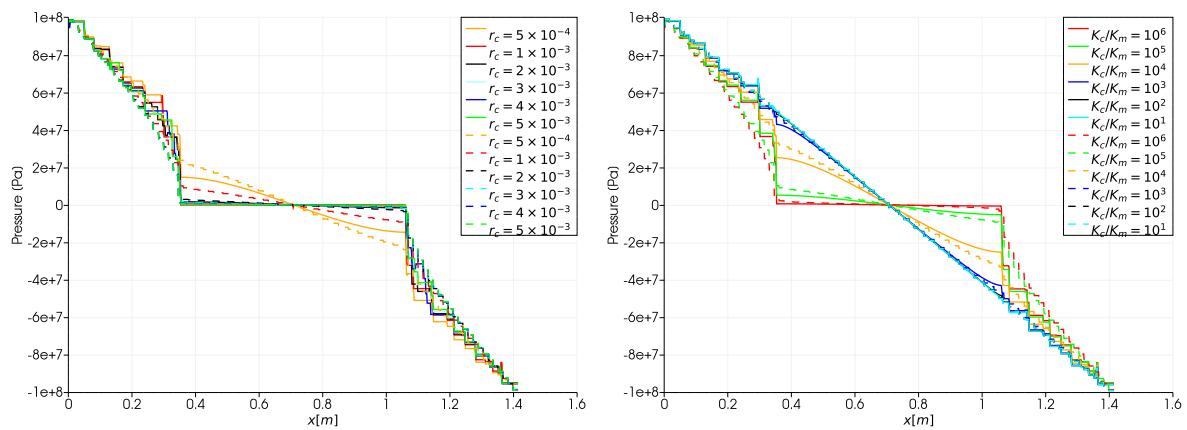


Figure 7. Pressure curves in the diagonal direction for the oblique conduit. Pressure distribution is shown for varying conduit radius (left) and permeability contrast (right). Continuous lines indicate the FEniCSx solutions, and dashed lines represent the finite volume formulation solutions.

Authorship statement. The authors hereby confirm that they are the sole liable persons responsible for the authorship of this work, and that all material that has been herein included as part of the present paper is either the property (and authorship) of the authors, or has the permission of the owners to be included here.

References

- [1] P. Ferraz, P. Pereira, E. Abreu, and M. A. Murad. Recursive mixed multiscale model reduction for karst conduit-flow in carbonate reservoirs. *Transport in Porous Media*, vol. 139, pp. 527–558, 2021.
- [2] I. Landim, M. A. Murad, P. Pereira, and E. Abreu. A new computational model for karst conduit flow in carbonate reservoirs including dissolution-collapse breccias. *Computational Geosciences*, vol. 27, pp. 879–912, 2023.
- [3] M. A. Murad, T. V. Lopes, P. A. Pereira, F. H. R. Bezerra, and A. C. Rocha. A three-scale index for flow in karst conduits in carbonate rocks. *Advances in Water Resources*, vol. 141, pp. 103613, 2020.
- [4] M. G. Correia, G. Oliveira, and D. J. Schiozer. Special connections for representing multiscale heterogeneities in reservoir simulation. *SPE Res Eval & Eng*, vol. 26, n. 04, pp. 1212–1223, 2023.
- [5] J. Cordazzo, C. R. Maliska, and A. F. C. Silva. Interblock transmissibility calculation analysis for petroleum reservoir simulation. *2nd Meeting on Reservoir Simulation*, vol. , 2002.
- [6] M. G. Correia, von J. C. Hohendorff Filho, and D. J. Schiozer. Multiscale integration for karst-reservoir flow-simulation models. *SPE Reservoir Evaluation & Engineering*, vol. 23, n. 02, pp. 518–533, 2020.
- [7] U. G. Moreira, F. F. Rocha, and F. S. Sousa. Investigation of a conservative finite volume scheme for flows in karstified porous media. *Proceeding Series of the Brazilian Society of Computational and Applied Mathematics*, vol. , n. In press, 2025.
- [8] H. P. Langtangen and A. Logg. *Solving PDEs in Python The FEniCS Tutorial I*. Springer Nature, 2017.
- [9] A. Dudun and Y. Feng. Modeling fluid flow in fractured porous media: a comparative analysis between darcy-darcy model and stokes-brinkman model. *J Petrol Explor Prod Technol*, vol. 14, pp. 909–926, 2024.
- [10] J. Zhang, R. Wang, Q. Xu, C. Lei, X. Yang, and X. Zheng. The investigation of fracture pattern effect on fluid transport and production prediction in m field. *Energy Exploration & Exploitation*, vol. 39, n. 5, pp. 1770–1785, 2021.
- [11] C. Wolfsteiner, L. J. Durlofsky, and K. Aziz. Calculation of well index for nonconventional wells on arbitrary grids. *Computational Geosciences*, vol. 7, n. 1, pp. 61–82, 2003.
- [12] U. G. Moreira, F. F. Rocha, A. Jaramillo, F. S. Sousa, R. F. Ausas, G. C. Buscaglia, and F. Pereira. Numerical solution of single-phase flows in karstified heterogeneous carbonate rocks. *Proceedings of the XLIII CILAMCE, ABMEC*, vol. , pp. 1–66, 2022.
- [13] F. F. Rocha, F. S. Sousa, R. F. Ausas, F. Pereira, and G. C. Buscaglia. Interface spaces based on physics for multiscale mixed methods applied to flows in fractured-like porous media. *Computer Methods in Applied Mechanics and Engineering*, vol. 385, pp. 114035, 2021.